Dynamic Uncertainty Set Characterization for Bulk Power Grid Flexibility Assessment

Farzaneh Pourahmadi, *Student Member, IEEE*, Houman Heidarabadi, *Student Member, IEEE*, Seyed Hamid Hosseini, *Member, IEEE*, and Payman Dehghanian, *Member, IEEE*

***Abstract*—The increasing variability of renewables and volatile chronological net-load in power grids engenders significant risks of an uncertain sufficiency of flexible capacity. Although considerable advances in power grid flexibility assessment have been made, modeling the effect of temporal correlations associated with wind generations on the system flexibility provision capability has remained a challenge. This paper proposes a novel UC-time-scale security-constrained affinely robust formulation for wind-originated uncertainty sets in order to evaluate the system flexibility capacity over time. An efficient model based on duality theorem and affine policy is proposed to assess a secure region in response to uncertain wind generation scenarios. A framework using a combination of column and constraint generation and alternative direction algorithms is then developed to solve the proposed optimization model. The impacts of the sequential nature of wind generation, a type of dynamic uncertainty set, on the worst cases of generating units' time-coupled ramping constraints are effectively captured to investigate how they contribute to the optimal allowable uncertainty set. Furthermore, the relationship between dynamic uncertainty set boundaries and the imposed re-dispatch costs are numerically investigated. Numerical experiments on the modified IEEE 73-bus test system reveals the efficacy of the suggested model and the proposed solution technique.**

***Index Terms*—Feasibility robustness, flexibility metrics, operational flexibility, optimal uncertainty set, robust optimization.**

NOMENCLATURE

Sets and Indices

I	Index for generating units.
W	Index for wind farms.
L	Index for transmission lines.
K	Index for loads.
T	Index for time periods.

Variables

$u_{\rm it}, v_{\rm it}$	Generating unit i's start up and shut down status in period t, respectively.
$x_{\rm it}$	Generating unit i's ON/OFF status in period t.
$pg_{\rm it}$	Active power of thermal generating unit i in period t.
pw_{wt}	Power output of wind farm w in period t.
$W_{wt}^{\rm UB}, W_{wt}^{\rm LB}$	Upper and lower bounds of the allowable wind generation interval of wind farm w in period t.
$\alpha_{\rm it}, \beta_{\rm it}$	The affine policy coefficients of unit i in period t.
ρ, γ	Dual variables used in the worst transmission constraints.
μ, υ	Dual variables used in the worst generation constraints.
λ	Dual variables used in the worst recourse cost constraint.
π, φ, ξ, ψ	Dual variables used in the worst ramp rate constraints.

Parameters

$\mathrm{MD}_i, \mathrm{MU}_i$	Minimum down and up time of generating unit i.
$\overline{pw}_{wt}$	Expected output of wind farm w in period t.
$\overline{pg}_{\rm it}, \overline{u}_{\rm it}, \overline{v}_{\rm it}$	Base point generation, started up, shut down status of generating unit i in period t.
RD_i, RU_i	Downward and upward ramping capability of generating unit i.
T	Number of time periods.
$W_{wt}^{\max}, W_{wt}^{\min}$	Upper and lower bounds of the predicted wind generation interval for wind farm w in period t.
H_l^i, H_l^w, H_l^k	Shift distribution factors of generator i, wind farm w, and load k with respect to line l.
$F_l^{\max}$	Transmission capacity of transmission line l.
pd_t^k	Demand in load point k in period t.
s_i^u	Start-up cost of generating unit i .
s_i^d	Shut-down cost of generating unit i.
c_i	Production cost function of generating unit i.
C_r	Upper limitation of recourse cost.
sc_w, lc_w	Coefficients of spillage and curtailment of a wind farm w, respectively.
$Pg_i^{\min}, Pg_i^{\max}$	Minimum and maximum output power of generating unit i.
$\Delta_{wt}^{\rm UB}, \Delta_{wt}^{\rm LB}$	Upper and lower bounds of wind generation temporal correlation of wind farm w between two time periods t and t-1.
ε_{wt}	Wind generation prediction errors of wind farm w in period t.

Manuscript received August 11, 2018; revised December 2, 2018; accepted February 12, 2019. Date of publication March 19, 2019; date of current version March 2, 2020. *(Corresponding author: Seyed Hamid Hosseini.)*

F. Pourahmadi, H. Heidarabadi, and S. H. Hosseini are with the Department of Electrical Engineering, Sharif University of Technology, Tehran 11365-11155, Iran (e-mail: Pourahmadi_f@ee.sharif.edu; hosseini@sharif.edu; heidarabadi_h@ee.sharif.edu).

P. Dehghanian is with the Department of Electrical and Computer Engineering, George Washington University, Washington, DC 20052 USA (e-mail: payman@gwu.edu).

Digital Object Identifier 10.1109/JSYST.2019.2901358

I. Introduction

WITH the rushing arrival of stochastic resources into power grids, more variability and uncertainty are embedded in the system's generation profile which has contributing to the advent of new challenges in the operation of power systems and management of energy markets, driving a need for greater flexibility requirements [1]–[5]. The notion of flexibility has recently attracted extensive attention in the power industry [6]. Flexibility assessments help planners to quantify the grid capacity to employ its flexible resources to accommodate and respond to a wide range of uncertain future conditions within an acceptable time window and cost [6].

The existing literature on the assessment of power system flexibility can be divided into two categories based on their target applications. One focuses on long-term planning whereas the other targets real-time operations [7]. In perspective of generation planning, a probabilistic metric, the so-called insufficient ramping resource expectation, is proposed in [8] to assess the flexibility insufficiency. In [9] and [10], flexibility is taken into account in long-term generation expansion planning based on an enhanced deterministic unit commitment (UC) model, yielding an optimal generation portfolio. In the short-term time-scale, ramping capacity and duration as well as energy storage capability are suggested in [11] as metrics for grid operational flexibility. In [12], an operational flexibility metric named lack of ramp probability is proposed to guarantee the sufficient ramp deliverability in real-time electricity markets. A robust model based on security-constrained multiperiod optimal power flow is proposed in [13] to evaluate the insufficient flexibility. Research efforts in [14] and [15] suggest a flexibility metric using robust optimization models to capture the do-not-exceed (DNE) limits for uncertainty set interval.

New operational challenges, e.g., insufficient minimum and maximum output limits, frequent start-ups and shut downs of generating units, shorter lead times, and increased ramping and reserve requirements due to unprecedented penetration of uncertain renewables can be all captured within the UC problem. The UC problem, if effectively formulated, can well represent the chronological net-load in the operational flexibility assessments [16]. In this context, a two-stage robust UC is a suitable and reliable tool as it can quantify the worst possible scenarios by capturing the variability and uncertainty of wind generation [17]–[22]. A concept based on the admissible uncertainty interval that the system can accommodate is proposed in [14], [15], [21]–[25]. In [14], [15], [24], and [25], the allowable interval for wind uncertainties is evaluated in economic dispatch (ED) scenarios, while such uncertainty set boundaries are found in the UC problems in [21]–[23] based on two-stage robust formulations. The worst wind scenarios are found in [21]–[23] according to vertices of the uncertainty set utilizing a position-based vertex method.

Based on a thorough survey of the literature, two concerns on the existing formulations for quantification of admissible uncertainty set exist. One challenge is to consider *temporal correlations* of uncertain wind generations due to the wind speed time dependency. It is, therefore, necessary to capture the time correlation impact of uncertainties on the worst-case scenarios of intertemporal constraints. In almost all former studies on power grid flexibility evaluations [14], [15], [21]–[25], a static uncertainty set has been adopted with ignored time-dependent correlations of renewables. To the best of the authors' knowledge, this is the first effort to assess the system flexibility capability through a robust UC formulation with a *dynamic uncertainty set* characterized as a decision variable.

The second challenge is investigating the economic impact of dynamic uncertainty set on the corrective actions of generating units, to realize economic allowable uncertainty boundaries. In [21]–[25], the effort is to minimize the operation cost in the here-and-now stage while ensuring the system security, where the effect of the re-dispatch costs on the optimal uncertainty set is ignored. While a cost limitation is set in [15] to control the operation cost under uncertainty, the framework is still based on the static uncertainty set and its application is limited to ED strategies.

Different from the past literature, this paper proposes a new adaptive robust optimization model within the UC framework to assess the DNE limits of a dynamic wind uncertainty set. In order to efficiently solve the proposed model, and different from the conventional decomposition methods, a new linear affine policy approach is proposed which not only accelerate the solution procedure but also captures the effect of temporal correlations of uncertain wind generations for more robust dispatch solutions. The proposed robust UC model with variable dynamic uncertainty interval is converted to a bilinear programming problem which is linearized utilizing column and constraint generation (C&CG) and alternative direction algorithms. The paper main contributions are listed as follows.

1) Different from the state-of-the-art models based on linear affine policy, a new adaptive robust UC optimization model and decision structure are proposed to assess the power grid operational flexibility. A fast, yet robust, solution technique through an efficient combination of the duality theorem, C&CG, and the alternative direction algorithm is developed to solve the proposed optimization model. The suggested technique ensures robustness and tractability of the dispatch and commitment solutions.
2) The effect of the time dependency of uncertain wind generations, a type of dynamic uncertainty set, on the worst-case scenarios of generating units' ramp rate constraints—inducing intertemporal coupling between dispatch decisions—is captured and embedded in the proposed robust UC model. The effect of wind correlation on the optimal boundaries of the allowable dynamic uncertainty set is quantified.
3) The economic impacts of re-dispatch corrective actions on the allowable interval of dynamic uncertainty set is quantified. The UC framework embedded with a dynamic uncertainty set ensures that the re-dispatch costs for all possible wind realizations are less than a prespecified threshold.

In the following, Sections II and III present the proposed mathematical formulations and solution technique, respectively.

Section IV is devoted to the numerical case studies and Section V narrates the concluding remarks.

II. Mathematical Formulation

An adaptive robust security constrained UC (SCUC) model is suggested that can capture the allowable boundaries of the uncertainty set. The proposed model quantifies the optimal uncertainty interval for wind generation and provides the optimal economic solutions for generating units to handle the wind variability and uncertainty. To find the operation schedule and the minimum and maximum allowable wind generations while satisfying system operation constraints under any realization of uncertain wind generation, the following optimization formulation is proposed.

A. Objective Function

Since the conservativeness of robust optimization models can be handled by adjusting the uncertainty set, the following objective function (1a) is to minimize the difference between the *optimal* and *forecasted* boundaries of the uncertainty set with respect to constraints (1b), (1c). Since the actual wind generation larger than the optimal upper boundary will cause wind spillage (WS) and the actual wind generation lower than the optimal lower boundary will lead to load curtailments, sc_w and lc_w are set to reflect the WS and load shedding (LS) costs, respectively. The solutions of the optimal uncertainty set can be used as the dispatch signals for wind farms in an ex-ante manner and determine a secure region for wind power utilization. Constraints (1b) and (1c) represent the limits on the uncertainty set boundaries

$$\min_{W^{\mathrm{UB}},W^{\mathrm{LB}}} \sum_t \sum_w \mathrm{sc}_w(W_{wt}^{\max} - W_{wt}^{\mathrm{UB}}) + lc_w(W_{wt}^{\mathrm{LB}} - W_{wt}^{\min}) \tag{1a}$$

$$\overline{pw}_{wt} \le W_{wt}^{\mathrm{UB}} \le W_{wt}^{\max} \quad \forall w, \forall t \tag{1b}$$

$$W_{wt}^{\min} \le W_{wt}^{\mathrm{LB}} \le \overline{pw}_{wt} \quad \forall w, \forall t. \tag{1c}$$

B. Generating Units' Constraints

$$-x_{i(t-1)} + x_{it} - x_{i\tau} \le 0 \quad \forall i, \forall t, \forall \tau \in \{t, ..., MU_i + t - 1\} \tag{1d}$$

$$x_{i(t-1)} - x_{it} + x_{i\tau} \le 1 \quad \forall i, \forall t, \forall \tau \in \{t, ..., MD_i + t - 1\} \tag{1e}$$

$$-x_{i(t-1)} + x_{it} - u_{it} \le 0 \quad \forall i, \forall t \tag{1f}$$

$$x_{i(t-1)} - x_{it} - v_{it} \le 0 \quad \forall i, \forall t \tag{1g}$$

$$x_{it}, u_{it}, v_{it} \in \{0, 1\} \quad \text{and} \quad x_{i0} = 0 \quad \forall i, \forall t \tag{1h}$$

$$Pg_i^{\min} x_{\mathrm{it}} \le pg_{\mathrm{it}} \le Pg_i^{\max} x_{\mathrm{it}} \quad \forall i, \forall t \tag{1i}$$

$$pg_{\mathrm{it}} - pg_{i(t-1)} \le x_{i(t-1)} RU_i + (1 - x_{i(t-1)}) Pg_i^{\min} \quad \forall i, \forall t \tag{1j}$$

$$pg_{i(t-1)} - pg_{\mathrm{it}} \le x_{\mathrm{it}} RD_i + (1 - x_{i(t-1)}) Pg_i^{\min} \quad \forall i, \forall t \tag{1k}$$

Constraints (1d)–(1h) are utilized to account for the minimum ON/OFF time (1d), (1e) as well as the units' start-up and shut-down states (1f), (1g). Constraint (1i) enforces the generation capacity limits of generating units and constraints (1j), (1k) restrict their ramping capacity.

C. System-Wide Constraints

$$-F_l^{\max} \le \sum_i H_l^i pg_{it} + \sum_w H_l^w pw_{wt} - \sum_k H_l^k pd_t^k) \le F_l^{\max} \quad \forall l, \forall t, \forall pw_{wt} \in [W_{wt}^{\mathrm{LB}}, W_{wt}^{\mathrm{UB}}] \tag{1l}$$

$$\sum_i pg_{it} + \sum_w pw_{wt} = \sum_k pd_t^k \quad \forall t, \forall pw_{wt} \in [w_{wt}^{\mathrm{LB}}, w_{wt}^{\mathrm{UB}}] \tag{1m}$$

$$\sum_t \sum_i c_i pg_{\mathrm{it}} + s_i^u u_{\mathrm{it}} + s_i^d v_{\mathrm{it}} \le \mathrm{C}_r. \tag{1n}$$

Constraints (1l), (1m) ensure the branch flow limits and nodal power balance under uncertain conditions. From (1l) and (1m), one can see that the realized schedule will be feasible for all wind realizations in the variable uncertainty set. Constraint (1n) restricts the cost associated with the base-case condition (with no uncertainty set characterization) and the recourse cost in face of uncertainties.

III. Solution Methodology

We propose an affine policy based approach that assumes a linear relationship for generating units' responses to the uncertain wind generation. The affine policy is employed to solve the robust optimization problem with *variable* uncertainty set—in contrast with the standard models with static uncertainty sets. Particularly, to simplify the problem and ensure its tractability, the following affine rule is assumed on the total output changes of variable resources [24]–[27]:

$$pg_{\mathrm{it}} = \alpha_{\mathrm{it}} + \beta_{\mathrm{it}} \sum_w pw_{wt} \tag{2}$$

where α_{it}^b and β_{it}^b are the affine policy coefficients. Using the linear affine dispatch policy (2), constraints (1i)–(1n) will have the following forms:

$$Pg_i^{\min} x_{\mathrm{it}} \le \alpha_{\mathrm{it}} + \beta_{\mathrm{it}} \sum_w pw_{wt} \le Pg_i^{\max} x_{\mathrm{it}} \quad \forall i, \forall t \tag{3a}$$

$$\alpha_{\mathrm{it}} + \beta_{\mathrm{it}} \sum_w pw_{wt} - \left(\alpha_{i(t-1)} + \beta_{i(t-1)} \sum_w pw_{w(t-1)}\right) \le x_{i(t-1)} RU_i + (1 - x_{i(t-1)}) Pg_i^{\min} \quad \forall i, \forall t, \forall pw_{wt} \tag{3b}$$

$$\alpha_{i(t-1)} + \beta_{i(t-1)} \sum_w pw_{w(t-1)} - \left(\alpha_{\mathrm{it}} + \beta_{\mathrm{it}} \sum_w pw_{wt}\right) \le x_{\mathrm{it}} RD_i + (1 - x_{i(t-1)}) Pg_i^{\min} \quad \forall i, \forall t, \forall pw_{wt} \tag{3c}$$

$$-F_l^{\max} \le \sum_i H_l^i \left(\alpha_{\rm it} + \beta_{\rm it} \sum_w pw_{wt}\right) + \sum_w H_l^w pw_{wt} - \sum_k H_l^k pd_t^k) \le F_l^{\max} \quad \forall l, \forall t, \forall pw_{wt} \tag{3d}$$

$$\sum_i \left(\alpha_{\rm it} + \beta_{\rm it} \sum_w pw_{wt}\right) + \sum_w pw_{wt} = \sum_k pd_t^k \quad \forall t, \forall pw_{wt} \tag{3e}$$

$$\sum_t \sum_i c_i \left(\alpha_{\rm it} + \beta_{it} \sum_w pw_{wt}\right) \le C_r \quad \forall pw_{wt}. \tag{3f}$$

Constraints (1i)–(1n) correspond to constraints (3), obtained by substituting pg_{it}^b with the affine policy (2). Note that constraints (3) are robust constraints that should hold for all $\forall pw_{wt} \in [W_{wt}^{\rm DN}, W_{wt}^{\rm UP}]$. Since the balance constraint (3e) holds for any uncertainty realization under the affine policy (2), the following equations should be satisfied:

$$\sum_i \beta_{it} = -1 \qquad \forall t \in T \tag{4a}$$

$$\sum_i \alpha_{it} = \sum_k pd_t^k \qquad \forall t \in T. \tag{4b}$$

Equation (4a) ensures that if there is a net decrease in wind generation, the units' outputs proportionally increase. Coefficient β_{it} reflects the participation factor of generating unit *i*; worthy to note that α_{it} can be considered as the base-point of generating unit *i*. In a robust optimization model, the worst-case scenario is typically a set of parameters such that security constraints for any other scenario can be guaranteed if and only if there exists a feasible solution under this scenario. Therefore, the analysis of possible worst-case wind scenarios is needed. While the affine policy approach is applied in [14], [24], and [25] to derive the worst-cases of transmission and generation constraints, we utilize it to model the worst re-dispatch cost and wind temporal correlations to characterize the optimal allowable uncertainty set. The following four worst-case scenarios should be satisfied for system security.

A. Worst-Case Scenarios of Operation Constraints

1) Transmission Constraints: Consider constraint (3d), which is actually equivalent to the following inequality constraint:

$$-F_l^{\max} \le \sum_i H_l^i \alpha_{\rm it} + \phi(\beta, W_{wt}^{DN}, W_{wt}^{UP}) - \sum_k H_l^k pd_t^k) \le F_l^{\max} \quad \forall l, \forall t, \forall pw_{wt} \tag{5a}$$

$$\phi(\beta, W_{wt}^{\rm DN}, W_{wt}^{\rm UP}) = \max_{pw_{wt}} \sum_i H_l^i \beta_{\rm it} \sum_w pw_{wt} + H_l^w pw_{wt}) \tag{5b}$$

and its corresponding dual problem can be expressed as

$$\min_{\rho^{\rm UP}\ge 0, \rho^{\rm DN}\ge 0} \sum_w (W_{wt}^{\rm UP} \rho_{w,l,t}^{\rm UP} - W_{wt}^{\rm DN} \rho_{w,l,t}^{\rm DN}) \tag{6a}$$

$$\rho_{w,l,t}^{\rm UP} - \rho_{w,l,t}^{\rm DN} = H_l^w + \sum_i H_l^i \beta_{\rm it} \qquad \forall w, \forall l, \forall t. \tag{6b}$$

By utilizing the strong duality theorem, constraint (6) is equivalent to the following set of constraints in (7):

$$\sum_w (W_{wt}^{\rm UP} \rho_{w,l,t}^{\rm UP} - W_{wt}^{\rm DN} \rho_{w,l,t}^{\rm DN}) + \sum_i H_l^i \alpha_{\rm it} - \sum_k H_l^k d_t^k \le F_l^{\max} \quad \forall l, \forall t \tag{7a}$$

$$\rho_{w,l,t}^{\rm UP} - \rho_{w,l,t}^{\rm DN} = H_l^w + \sum_i H_l^i \beta_{\rm it} \quad \forall w, \forall l, \forall t \tag{7b}$$

$$\rho_{w,l,t}^{\rm UP} \ge 0, \rho_{w,l,t}^{\rm DN} \ge 0 \quad \forall l, \forall t \tag{7c}$$

$$\sum_w (W_{wt}^{\rm UP} \gamma_{w,l,t}^{\rm UP} - W_{wt}^{\rm DN} \gamma_{w,l,t}^{\rm DN}) - \sum_i H_l^i \alpha_{\rm it} + \sum_k H_l^k d_t^k \le -F_l^{\max} \quad \forall l, \forall t \tag{7d}$$

$$\gamma_{w,j,t}^{\rm UP} - \gamma_{w,j,t}^{\rm DN} = -H_l^w - \sum_i H_l^i \beta_{\rm it} \quad \forall w, \forall l, \forall t \tag{7e}$$

$$\gamma_{w,l,t}^{\rm UP} \ge 0, \ \gamma_{w,l,t}^{\rm DN} \ge 0 \qquad \forall l, \forall w. \tag{7f}$$

2) Generation Constraints: Using the same technique, it can be shown that constraint (3a) is equivalent to the following set of constraints in (8):

$$\alpha_{\rm it} + \sum_w (W_{wt}^{\rm UP} \mu_{w,i,t}^{\rm UP} - W_{wt}^{\rm DN} \mu_{w,i,t}^{\rm DN}) \le Pg_i^{\max} x_{\rm it} \quad \forall i, \forall t \tag{8a}$$

$$\mu_{w,i,t}^{\rm UP} - \mu_{w,i,t}^{\rm DN} = \beta_{\rm it} \qquad \forall w, \forall i, \forall t \tag{8b}$$

$$\mu_{w,i,t}^{\rm DN} \ge 0, \mu_{w,i,t}^{\rm DN} \ge 0 \qquad \forall w, \forall i, \forall t \tag{8c}$$

$$-\alpha_{\rm it} + \sum_w (w_{wt}^{\rm UP} \upsilon_{w,i,t}^{\rm UP} - w_{wt}^{\rm DN} \upsilon_{w,i,t}^{\rm DN}) \le -Pg_i^{\min} x_{\rm it} \quad \forall i, \forall t \tag{8d}$$

$$\upsilon_{w,i,t}^{\rm UP} - \upsilon_{w,i,t}^{\rm DN} = -\beta_{\rm it}, \qquad \forall w, \forall i, \forall t \tag{8e}$$

$$\upsilon_{w,i,t}^{\rm UP} \ge 0, \ \upsilon_{w,i,t}^{\rm DN} \ge 0 \qquad \forall w, \forall i, \forall t. \tag{8f}$$

3) Recourse Cost Constraints: Similarly, constraint (3f) can be written as follows:

$$\sum_t \sum_i c_i \alpha_{\rm it} + \sum_w (W_{wt}^{\rm UP} \lambda_{w,t}^{\rm UP} - W_{wt}^{\rm DN} \lambda_{w,t}^{\rm DN}) \le C_r \quad \forall i, \forall t \tag{9a}$$

$$\lambda_{w,t}^{\rm UP} - \lambda_{w,t}^{\rm DN} = \beta_{\rm it} \quad \forall w, \forall t. \tag{9b}$$

4) Ramp Rate Constraints: The ramping constraints reflect decisions over consecutive time periods, i.e., the induced intertemporal coupling between dispatch decisions. Therefore, different from transmission, generation, and recourse cost constraints, the intertemporal correlation of wind generations is considered to characterize the worst-case scenario of ramp rate constraints in (10c)

$$W_{wt}^{\rm LB} \le pw_{wt} \le W_{wt}^{\rm UB} \quad \forall w, \forall t \tag{10a}$$

$$W_{w(t-1)}^{\rm LB} \le pw_{w(t-1)} \le W_{w(t-1)}^{\rm UB} \quad \forall w, \forall t \tag{10b}$$

$$\Delta_{wt}^{\rm LB} \le pw_{wt} - pw_{w(t-1)} \le \Delta_{wt}^{\rm UB} \quad \forall w, \forall t. \tag{10c}$$

For simplicity, we consider the correlation of uncertain wind generations between two consecutive time periods to reflect the effect of dynamic uncertainty set on intertemporal robust constraints; the proposed framework is generic to accommodate additional intertemporal constraints. As a result of the uncertainty set in (10), the intertemporal robust constraints in (3b) and (3c) are equivalent to the vectors $\pi^{\mathrm{UB}}, \pi^{\mathrm{LB}}, \varphi^{\mathrm{UB}}, \varphi^{\mathrm{LB}}, \xi^{\mathrm{UB}}, \xi^{\mathrm{LB}}, \psi^{\mathrm{UB}}, \psi^{\mathrm{LB}} \geq 0$ such that

$$\begin{aligned} & W_{wt}^{\mathrm{UB}}\pi_{w,i,t}^{\mathrm{UB}} - W_{wt}^{\mathrm{LB}}\pi_{w,i,t}^{\mathrm{LB}} + W_{w(t-1)}^{\mathrm{UB}}\pi_{w,i,(t-1)}^{\mathrm{UB}} \\ & \quad - W_{w(t-1)}^{\mathrm{LB}}\pi_{w,i,(t-1)}^{\mathrm{LB}} + \Delta_{wt}^{\mathrm{UB}}\varphi_{w,i,t}^{\mathrm{UB}} - \Delta_{wt}^{\mathrm{LB}}\varphi_{w,i,t}^{\mathrm{LB}} \\ & \quad \leq \alpha_{i(t-1)} - \alpha_{\mathrm{it}} + x_{i(t-1)}RU_i \\ & \quad + (1 - x_{i(t-1)})Pg_i^{\min} \quad \forall i, \forall t \end{aligned} \tag{11a}$$

$$\pi_{w,i,t}^{\mathrm{UB}} - \pi_{w,i,t}^{\mathrm{LB}} + \varphi_{w,i,t}^{\mathrm{UB}} - \varphi_{w,i,t}^{\mathrm{LB}} = \beta_{\mathrm{it}} \quad \forall i, \forall t \tag{11b}$$

$$\pi_{w,i,(t-1)}^{\mathrm{UB}} - \pi_{w,i,(t-1)}^{\mathrm{LB}} - \varphi_{w,i,t}^{\mathrm{UB}} + \varphi_{w,i,t}^{\mathrm{LB}} = -\beta_{\mathrm{it}} \quad \forall i, \forall t \tag{11c}$$

$$\begin{aligned} & W_{wt}^{\mathrm{UB}}\xi_{w,i,t}^{\mathrm{UB}} - W_{wt}^{\mathrm{LB}}\xi_{w,i,t}^{\mathrm{LB}} + w_{w(t-1)}^{\mathrm{UB}}\xi_{w,i,(t-1)}^{\mathrm{UB}} \\ & \quad - w_{w(t-1)}^{\mathrm{LB}}\xi_{w,i,(t-1)}^{\mathrm{LB}} + \Delta_{wt}^{\mathrm{UB}}\psi_{w,i,t}^{\mathrm{UB}} - \Delta_{wt}^{\mathrm{LB}}\psi_{w,i,t}^{\mathrm{LB}} \\ & \quad \leq \alpha_{\mathrm{it}} - \alpha_{i(t-1)}x_{\mathrm{it}}RD_i \\ & \quad + (1 - x_{i(t-1)})Pg_i^{\min} \quad \forall i, \forall t \end{aligned} \tag{11d}$$

$$\xi_{w,i,t}^{\mathrm{UB}} - \xi_{w,i,t}^{\mathrm{LB}} + \psi_{w,i,t}^{\mathrm{UB}} - \psi_{w,i,t}^{\mathrm{LB}} = -\beta_{\mathrm{it}} \quad \forall i, \forall t \tag{11e}$$

$$\xi_{w,i,(t-1)}^{\mathrm{UB}} - \xi_{w,i,(t-1)}^{\mathrm{LB}} - \psi_{w,i,t}^{\mathrm{UB}} + \psi_{w,i,t}^{\mathrm{LB}} = \beta_{\mathrm{it}} \quad \forall i, \forall t. \tag{11f}$$

B. Proposed Compact Model and Algorithm

With the equivalent constraints in face of uncertainties, the optimization problem (1) is converted to a bilinear problem (1b)–(1h), (4), (7)–(9), (11). The following compact matrix formulation is presented for each time interval *t*:

$$\min_{\substack{W^{\mathrm{LB}}, W^{\mathrm{UB}} \\ \eta, \phi, \delta, \alpha}} \quad lc^T(W^{\mathrm{LB}} - W^{\min}) + \mathrm{sc}^T(W^{\max} - W^{\mathrm{UB}}) \tag{12a}$$

$$\text{s.t. } AX \leq b \tag{12b}$$

$$\eta^{\mathrm{UB}}W^{\mathrm{UB}} + \eta^{\mathrm{LB}}W^{\mathrm{LB}} \leq DX + E\alpha + Fd + g \tag{12c}$$

$$\eta^{\mathrm{UB}} - \eta^{\mathrm{LB}} = I\beta + H \tag{12d}$$

$$\phi^{\mathrm{UB}}W^{\mathrm{UB}} + \phi^{\mathrm{LB}}W^{\mathrm{LB}} + \delta^{\mathrm{UB}}\Delta^{\mathrm{UB}} + \delta^{\mathrm{LB}}\Delta^{\mathrm{LB}} \leq BX + C\alpha \tag{12e}$$

$$\phi^{\mathrm{UB}} - \phi^{\mathrm{LB}} + P\delta^{\mathrm{UB}} + Q\delta^{\mathrm{LB}} = S\beta \tag{12f}$$

$$Jw^{\mathrm{UB}} + Kew + Lw^{\max} \leq f \tag{12g}$$

$$Mw^{\mathrm{LB}} + Rew + Nw^{\min} \leq h \tag{12h}$$

$$1^T\alpha = 1^Td \tag{12i}$$

$$1^T\beta = -1. \tag{12j}$$

Constraint (12b) is the closed-form of (1d)–(1h). Similarly, constraints (12c–(12j) represent the closed-forms of (7)–(9), (11), (1b), (1c), (4a), and (4b), respectively. As dual variables and lower and upper bounds of uncertainty set are multiplied in (12c)–(12e), a bilinear model exists in which the participation factors, dual variables and the uncertainty set intervals are optimized. Regarding constraint (12d), if the participation factor matrix β is fixed at certain values of β^*, constraint (12c) will be converted to a linear one as follows:

$$\eta^{\mathrm{UB}*}W^{\mathrm{UB}} + \eta^{\mathrm{LB}*}W^{\mathrm{LB}} \leq DX + E\alpha + Fd + g \tag{13a}$$

$$\eta^{\mathrm{UB}*} = \max(0, I\beta^* + H) \tag{13b}$$

$$\eta^{\mathrm{LB}*} = -\min(0, I\beta^* + H). \tag{13c}$$

Even with a fixed participation factorβ, constraint (12e) remains bilinear due to the additional terms of $P\delta^{\mathrm{UB}}$ and $Q\delta^{\mathrm{LB}}$ in (12f). To linearize the constraint, we apply the proposed solution algorithm based on C&CG and alternating direction algorithms.

In the proposed solution algorithm, the master problem (15) is solved repeatedly while considering the dual variables fixed as parameters; we systematically improve the scaling dual parame-

---

The proposed Algorithm for Quantification of Optimal Uncertainty Set.

Step 1. Set the initial value for uncertainty set boundaries $\boldsymbol{W^{UB*}} = \boldsymbol{W}^{\max}$ and $\boldsymbol{W^{LB*}} = \boldsymbol{W^{LB}}$. Set $\boldsymbol{Q} = +\infty$, $\boldsymbol{q} = -\infty$, and $\boldsymbol{k} = \boldsymbol{1}$.

Step 2. Solve the linear problem (14), get the optimal solutions of $\boldsymbol{\phi^{UB*}}$, $\boldsymbol{\phi^{LB*}}$, $\boldsymbol{\delta^{UB*}}$ and $\boldsymbol{\delta^{LB*}}$.

$$\begin{aligned} \boldsymbol{z} = \min\ & \boldsymbol{\phi^{UB}W^{UB*}} + \boldsymbol{\phi^{LB}W^{LB*}} \\ & + \boldsymbol{\delta^{UB}}\Delta^{UB} + \boldsymbol{\delta^{LB}}\Delta^{LB} \\ \text{s.t. } & \boldsymbol{\phi^{UB}} - \boldsymbol{\phi^{LB}} + \boldsymbol{P\delta^{UB}} + \boldsymbol{Q\delta^{LB}} = \boldsymbol{S\beta} \end{aligned} \tag{14}$$

Update $\boldsymbol{Q} = \boldsymbol{z} + \boldsymbol{lc^T}(\boldsymbol{W^{LB*}} - \boldsymbol{W}^{\min})$ $+\boldsymbol{sc^T}(\boldsymbol{W}^{\max} - \boldsymbol{W^{UB*}})$.

Step 3. Solve the mixed integer linear programming (15) with the obtained $\boldsymbol{\eta_k^{UB*}}$ and $\boldsymbol{\eta_k^{LB*}}$ from (13b), (13c) and the optimal solutions of $\boldsymbol{\phi_k^{UB*}}$, $\boldsymbol{\phi_k^{LB*}}$, $\boldsymbol{\delta_k^{UB*}}$, and $\boldsymbol{\delta_k^{LB*}}$ from (14) at iteration **k**.

$$\begin{aligned} \boldsymbol{Z} = \min_{\alpha, \boldsymbol{X}, \boldsymbol{W^{UB}}, \boldsymbol{W^{LB}}}\ & \boldsymbol{lc^T}(\boldsymbol{W^{LB}} - \boldsymbol{W}^{\min}) \\ & + \boldsymbol{sc^T}(\boldsymbol{W}^{\max} - \boldsymbol{W^{UB}}) + \boldsymbol{\theta} \end{aligned} \tag{15}$$

s.t. (12b), (12g)–(12i)

$\boldsymbol{\eta_k^{UB*}}\ \boldsymbol{W^{UB}} + \boldsymbol{\eta_k^{LB*}}\ \boldsymbol{W^{LB}} \leq \boldsymbol{DX} + \boldsymbol{E\alpha} + \boldsymbol{Fd} + \boldsymbol{g}$

$\boldsymbol{\phi_k^{UB*}}\ \boldsymbol{W^{UB}} + \boldsymbol{\phi_k^{LB*}}\ \boldsymbol{W^{LB}} + \boldsymbol{\delta_k^{UB*}}\Delta^{UB}$ $+\boldsymbol{\delta_k^{LB*}}\Delta^{LB} \leq \boldsymbol{BX} + \boldsymbol{C\alpha}$

$\boldsymbol{\theta} \leq\ \boldsymbol{\phi_k^{UB*}}\ \boldsymbol{W^{UB}} + \boldsymbol{\phi_k^{LB*}}\ \boldsymbol{W^{LB}}$ $+\boldsymbol{\delta_k^{UB*}}\Delta^{UB} + \boldsymbol{\delta_k^{LB*}}\Delta^{LB}$

Obtain the optimal value of $\boldsymbol{Z}^*$ and update $\boldsymbol{q} = \boldsymbol{Z}^*$.

Step 4. If $\boldsymbol{Q} - \boldsymbol{q} \leq \varepsilon$, return optimal boundaries of uncertainty set, otherwise return $\boldsymbol{W^{UB*}}$ and $\boldsymbol{W^{LB*}}$, set **k** $=$ **k** $+$ **1**, and go to **Step 2**.

---

ters by solving the sub-problem (14). The main idea behind this approach is inspired by the main principles of the C&CG and alternative algorithms [18], [28]. In order to shrink the feasible region of the master problem (15), the cuts corresponding to the optimal dual variables captured in sub-problem (14) are added to the master problem at each iteration. Similar to the CCG and Benders decomposition techniques [18], [28], the upper and lower bounds of the proposed algorithm are attributed to a decreasing and increasing characteristic, respectively. Therefore, it will converge to an optimal solution within a finite number of iterations, if the master problem becomes feasible at all iterations. It is worth pointing out that, in some cases, the algorithm cannot find the optimal solution since the master problem becomes infeasible due to the ramp rate constraints with bilinear terms (that is, for lower values of U, the corresponding dual variables $\varphi^{\mathrm{UB}}_{w,i,t}$ and $\psi^{\mathrm{UB}}_{w,i,t}$ will be large in the sub-problem, resulting in infeasibility of the ramp rate constraints corresponding to system generating units). In this regard, the infeasibility degree can be defined by the following equations:

$$\begin{aligned}\text{Ramp-up}^{\inf}_{\mathrm{i,t}} &= RU_i \\ &\quad - \sum_{w\in W}\left(\Delta^{\mathrm{UB}}_{wt}\varphi^{\mathrm{UB}}_{w,i,t} - \Delta^{\mathrm{LB}}_{wt}\varphi^{\mathrm{LB}}_{w,i,t}\right) \quad \forall i, \forall t \\ \text{Ramp-dn}^{\inf}_{\mathrm{i,t}} &= RD_i \\ &\quad - \sum_{w\in W}\left(\Delta^{\mathrm{UB}}_{wt}\psi^{\mathrm{UB}}_{w,i,t} - \Delta^{\mathrm{LB}}_{wt}\psi^{\mathrm{LB}}_{w,i,t}\right) \quad \forall i, \forall t.\end{aligned} \tag{16}$$

Should any parts of the above-mentioned parameters be positive, the ramp constraints will be feasible for the corresponding generating unit and the time interval.

In summary, the proposed flexibility evaluation framework is architecturally presented in Fig. 1. In Stage I, the required data on the system transmission lines, generating units, loads, and wind generation profile are collected and populated in the proposed toolset. In Stage II, the worst-case scenarios for the flexibility assessment problem (3) are defined through a joint utilization of the duality theory and an affine policy-based strategy. In Stage III, the proposed approach for flexibility assessment (12) is formulated as a bilinear problem due to the intertemporal constraints associated with the ramp rate limitations of generating units. To linearize the optimization problem, the aforementioned algorithm based on C&CG and alternating direction methods is applied to characterize the optimal dynamic uncertainty set which reflects the effect of temporal correlation of wind generations on the flexibility capacity of the system at any given point in time.

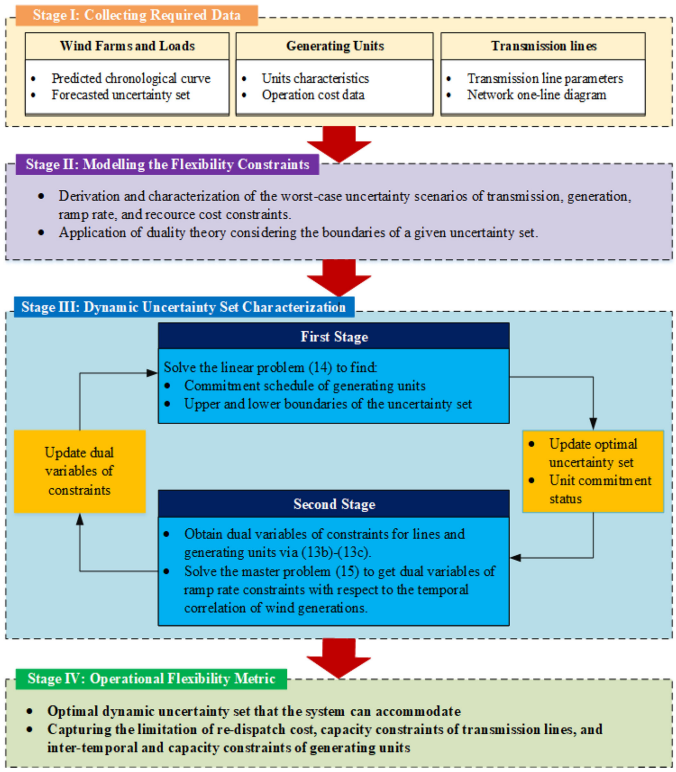

Fig. 1. Proposed operational flexibility assessment method scheme.

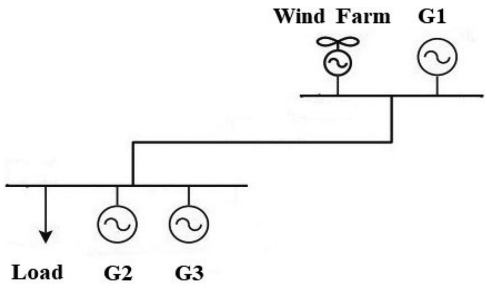

Fig. 2. Two-bus test system with integrated wind farms.

IV. Numerical Analysis

A. Case Study 1: Demonstrative Example

The small test system here integrates three conventional generating units, one wind power plant, and one load point, as shown in Fig. 2. In order to demonstrate the effect of time correlations associated with wind generation, we consider two time intervals. Generating unit data, expected wind farm generation and load point demand are given in Tables I and II, respectively. For the sake of simplicity, transmission power flow limitations are neglected in this example. The forecast error is assumed to be 50%. The proposed model is applied considering the time correlation constraint (10c) with $\Delta^{\mathrm{UB}} = 20$ and $\Delta^{\mathrm{LB}} = -20$ is converged in four iterations. The feasible regions for W_t^{UB} and

TABLE I
Generating Unit Data

Unit	c_i ($/MWh)	$Pg_i^{\min}$ (MW)	$Pg_i^{\max}$ (MW)	RU_i (MW/h)	RD_i (MW/h)	s_i^u ($)	s_i^d ($)
G1	10	15	50	20	15	0	0
G2	30	10	80	10	10	50	0
G3	35	10	90	10	10	10	0

TABLE II
LOAD POINT DEMAND AND WIND FARM DATA

Time interval	t_1	t_2
$\overline{pw}_t$ (MW)	10	50
pd_t (MW)	50	100

W_t^{LB} are determined by (17)

$$0 \le W_{t1}^{\mathrm{UB}} \le 5 \tag{17a}$$

$$0 \le W_{t2}^{\mathrm{UB}} \le 25 \tag{17b}$$

$$-5 \le W_{t1}^{\mathrm{LB}} \le 0 \tag{17c}$$

$$-25 \le W_{t2}^{\mathrm{LB}} \le 0 \tag{17d}$$

$$W_{t1}^{\mathrm{UB}} - 0.75\, W_{t2}^{\mathrm{LB}} \le 15.833 \tag{17e}$$

$$W_{t2}^{\mathrm{LB}} \ge -16.67 \tag{17f}$$

$$W_{t2}^{\mathrm{UB}} \le 18.33. \tag{17g}$$

Constraints (17a)–(17d) limit the uncertainty deviations. Constraint (17e) is generated in the second iteration via the worst-case scenario of ramp-up constraint (11a) where the dual variables corresponding to the upper and lower bounds of (10a) are equal to 1 and 0.75, respectively, and those of constraint (10c) are zero. In the other iteration, the dual variables related to constraint (10c) are activated which affect directly the optimal value of α_{it} and indirectly the feasible region. The worst case scenario of the upper and lower bound generation capacity of generating unit G_1 at t_2 in the first iteration engenders the lower bound of W_{t2}^{LB} [constraint (17f)] and upper bound W_{t2}^{UB} [constraint (17e)], respectively. Upon convergence, the solution vector of the allowable upper and lower bounds in two time intervals is obtained as follows:

$$(W_{t1}^{\mathrm{UB}}, W_{t1}^{\mathrm{LB}}, W_{t2}^{\mathrm{UB}}, W_{t2}^{\mathrm{LB}}) = (3.33, -5, 18.33, -16.67). \tag{18}$$

Note that in the first iteration, only generating unit G_1 meets the demand at t_1 and t_2 and, hence, its participation factor is 1; however, in the 2nd, 3rd, and 4th iterations, generating unit G_2 is activated at t_1 and t_2. Thus, participation factors of G_1 and G_2 in the last three iterations are 0.75 and 0.25, respectively.

B. Effect of Time Correlation Between Two Consecutive Wind Generations

In order to further validate the proposed approach, the performance of the suggested flexibility measure is compared with the *static* model based on [14] and [15] in which the temporal correlation of uncertain wind productions over consecutive time intervals is ignored. In other words, in the static model, the proposed ramping constraints of generating units (11a)–(11f) which induce intertemporal coupling between dispatch decisions in the UC problem are reformulated as

$$\begin{aligned} &W_{wt}^{\mathrm{UB}}\pi_{w,i,t}^{\mathrm{UB}} - W_{wt}^{\mathrm{LB}}\pi_{w,i,t}^{\mathrm{LB}} \\ &+ W_{w(t-1)}^{\mathrm{UB}}\pi_{w,i,(t-1)}^{\mathrm{UB}} - W_{w(t-1)}^{\mathrm{LB}}\pi_{w,i,(t-1)}^{\mathrm{LB}} \\ &\le \alpha_{i(t-1)} - \alpha_{\mathrm{it}} + x_{i(t-1)}RU_i + (1 - x_{i(t-1)})Pg_i^{\min} \quad \forall i, \forall t \end{aligned} \tag{19a}$$

$$\pi_{w,i,t}^{\mathrm{UB}} - \pi_{w,i,t}^{\mathrm{LB}} = \beta_{\mathrm{it}} \quad \forall i, \forall t \tag{19b}$$

$$\pi_{w,i,(t-1)}^{\mathrm{UB}} - \pi_{w,i,(t-1)}^{\mathrm{LB}} = -\beta_{\mathrm{it}} \quad \forall i, \forall t \tag{19c}$$

$$\begin{aligned} &W_{wt}^{\mathrm{UB}}\xi_{w,i,t}^{\mathrm{UB}} - W_{wt}^{\mathrm{LB}}\xi_{w,i,t}^{\mathrm{LB}} \\ &+ w_{w(t-1)}^{\mathrm{UB}}\xi_{w,i,(t-1)}^{\mathrm{UB}} - w_{w(t-1)}^{\mathrm{LB}}\xi_{w,i,(t-1)}^{\mathrm{LB}} \\ &\le \alpha_{\mathrm{it}} - \alpha_{i(t-1)} + x_{\mathrm{it}}RD_i + (1 - x_{i(t-1)})Pg_i^{\min} \quad \forall i, \forall t \end{aligned} \tag{19d}$$

$$\xi_{w,i,t}^{\mathrm{UB}} - \xi_{w,i,t}^{\mathrm{LB}} = -\beta_{\mathrm{it}} \quad \forall i, \forall t \tag{19e}$$

$$\xi_{w,i,(t-1)}^{\mathrm{UB}} - \xi_{w,i,(t-1)}^{\mathrm{LB}} = \beta_{\mathrm{it}} \quad \forall i, \forall t. \tag{19f}$$

To derive this reformulation, the temporal correlation of wind generations (10c) is neglected. Considering relatively little work published on the characterization of the optimal adjustable uncertainty set in UC time scale using affine policy, we extend the approach in [14] and [15] to the UC problem in order to fairly compare its performance with our proposed model. Research efforts in [14] and [15] evaluate the allowable interval for wind uncertainties in the ED problem. Therefore, we add the binary variables of generating units' commitment and extend its constraints to 24 h. Hence, the static model results in the feasible region to be modified as follows:

$$\text{(17a)–(17d)}$$

$$W_{t1}^{\mathrm{UB}} - W_{t2}^{\mathrm{LB}} \le 21.75 \tag{20a}$$

$$W_{t2}^{\mathrm{UB}} - W_{t1}^{\mathrm{LB}} \le 13.25 \tag{20b}$$

$$W_{t2}^{\mathrm{UB}} \le 12. \tag{20c}$$

The generating unit ramp-up constraint (19a) in the 1st iteration forms the constraint (20a) in which the dual variable of constraints (10a) is equal to 1, since the dual variable of constraint (10c) is 0. Constraint (20b) is formed by the worst case scenario of ramp-down constraint (19d). Similarly, the dual variable of constraint (10a) utilized in (19d) is equal to 1. The worst case of the lower bound for generating unit G_1 capacity at t_2 in the first iteration creates the upper limit W_{t2}^{UB}. Regarding the feasible region in (17a)–(17d) and (20a)–(20c), the solution vector for the allowable upper and lower bounds is obtained as follows:

$$(W_{t1}^{\mathrm{UB}}, W_{t1}^{\mathrm{LB}}, W_{t2}^{\mathrm{UB}}, W_{t2}^{\mathrm{LB}}) = (5, -1.25, 12, -16.75). \tag{21}$$

When ignoring the time correlation of wind generation, only generating unit G_1 meets the demand in the 1st iteration, whereas in the next iterations, generating unit G_2 at t_1 and t_2 and generating unit G_3 at t_2 are activated with participation factors assigned

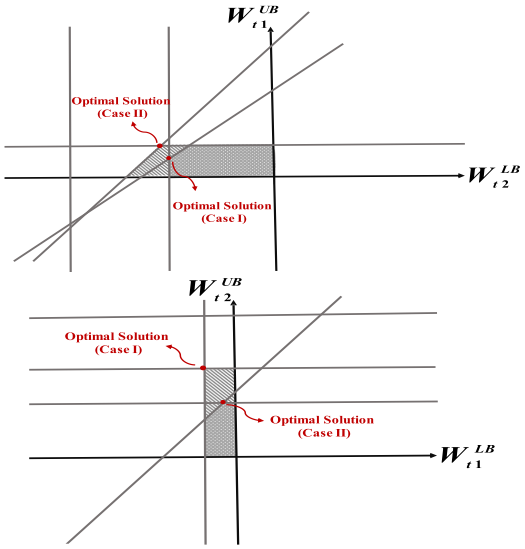

Fig. 3. Effect of wind generation temporal correlation on feasible region and optimal solution.

as follows:

$$(\beta_{i1,t1}, \beta_{i2,t1}, \beta_{i1,t2}, \beta_{i2,t2}, \beta_{i3,t2}) = (0.75, 0.25, 0.62, 0.20, 0.18). \quad (22)$$

Fig. 3 illustrates how the time correlation of wind generations in two time intervals affects not only the feasible region but also the corner points and optimal solution. In case I, the time correlation of the wind generations at t_1 and t_2 is considered, while in case II, it is assumed that the wind generations in the two time intervals are not correlated and the solution is provided by the static model.

1) Effect of Minimum Up/Down Time of Generating Units: Earlier, we demonstrated the impact of time correlation on the optimal solution. In this section, the minimum up and down time constraints of generating units are included to demonstrate how they impact the optimal solutions. Here, it is supposed that the minimum up and down times for all system generating units are equal to 2 h. The calculated upper and lower bounds for the uncertainty set are assessed as follows:

$$(W_{t1}^{\mathrm{UB}}, W_{t1}^{\mathrm{LB}}, W_{t2}^{\mathrm{UB}}, W_{t2}^{\mathrm{LB}}) = (5, -5, 18.75, -16.25). \quad (23)$$

The proposed algorithm is converged in the 2nd iteration. One can see that the minimum up and down time constraints of system generating units contribute to the commitment decisions of the units which in turn, affect the value of β_{it}. Consequently, they also affect the dual variables. Hence, the optimality cuts, and subsequently the feasible region for the calculated upper and lower bounds, are entirely distinct when such minimum up and down constraints are included compared to that when such constraints are ignored.

C. Case Study 2: IEEE RTS-96 Test System

The modified IEEE RTS-96 test system consists of 73 buses, 96 generating units, 51 load points, 120 transmission lines, 19 wind farms, and 40 storage units [29], [30]. The total installed capacity of wind farms and storage units are 6900 MW and 1280 MW, respectively. The generating unit data and wind farm parameters are borrowed from [30] and [31]. The ramping capability of generating units is reduced to 75% of the original values. The proposed approach is implemented in GAMS 24.1 platform using CPLEX 12.1 solver, on an Intel(R) Core i7 CPU (2.67 GHZ) with 4 GB memory.

1) Impact of Wind Generation Temporal Correlation on Optimal Uncertainty Interval: With a forecasted uncertainty set of wind generation as the input, the proposed robust optimization model is applied to the test system to characterize the largest uncertainty interval that the system can accommodate. In the proposed model, the coefficients sc_w and lc_w corresponding to the WS and LS costs are set to 10 and 1000, respectively. Here, the impact of temporal correlations [see constraint (10)] of wind generations on the flexibility and uncertainty set interval is studied. We consider three scenarios where three different values for the upper and lower limitations of (10c) are enforced and one scenario of the static model in which constraint (10c) is neglected. The uncertainty of wind generation, the deviation of wind power from its expected value, is assumed to be 20% [21]. The bounds for the predicted uncertainty set and those considering the time correlation between two consecutive wind generations are selected as follows:

$$W_{wt}^{\max} = 1.2 \times \overline{\mathrm{PW}}_{wt}, \; W_{wt}^{\min} = 0.8 \times \overline{\mathrm{PW}}_{wt} \quad \forall w, \forall t \quad (24a)$$

$$\Delta_{wt}^{\mathrm{UB}} = (W_{wt}^{\max} - W_{w(t-1)}^{\min}) \times U \quad \forall w, \forall t \quad (24b)$$

$$\Delta_{wt}^{\mathrm{LB}} = (W_{wt}^{\min} - W_{w(t-1)}^{\max}) \times U \quad \forall w, \forall t. \quad (24c)$$

In order to linearize nonlinear constraints (7)–(9), we consider the predefined participation factors given in (25) and the proposed solution algorithm

$$\beta_{\mathrm{it}} = -\left(\frac{x_{\mathrm{it}}}{c_i}\right) \cdot \left(\sum_i \left(\frac{x_{\mathrm{it}}}{c_i}\right)\right)^{-1} \quad \forall i, \forall t \quad (25)$$

where c_i is the production cost function of generating unit *i*. In the proposed algorithm, x_{it} and β_{it} are updated in the first stage at each iteration. The proposed robust model will yield a quantified optimal uncertainty set and the dual variables of constraints (10). Fig. 4 depicts the optimal interval for the uncertainty set in three scenarios of $U = 100\%$, 90%, and 80%, and for the scenario where constraint (10c) is neglected. As it can be seen in Fig. 4, the optimal uncertainty interval in the test scenario of $U = 100\%$ is equal to that when the temporal correlation constraint (10c) is neglected. That is due to the fact that if U is selected as 1 in constraints (24b), (24c), constraint (10c) can be obtained from constraints (10a), (10b); therefore, it can be ignored from the proposed model.

To demonstrate the effect of wind time-correlation on the optimal boundaries of the uncertainty set that the system can accommodate, Fig. 5 illustrates the comparison results of the optimal upper and lower bounds provided by the proposed model with $U = 90\%$ and the static model in [14] and [15]. The optimal boundaries obtained from these two models at hours 13–24 are

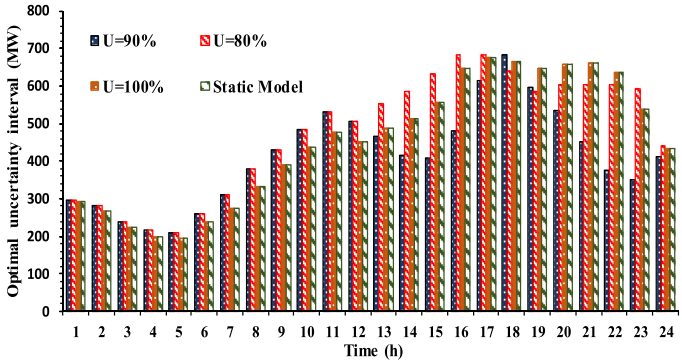

Fig. 4. Optimal uncertainty set intervals in different scenarios of U.

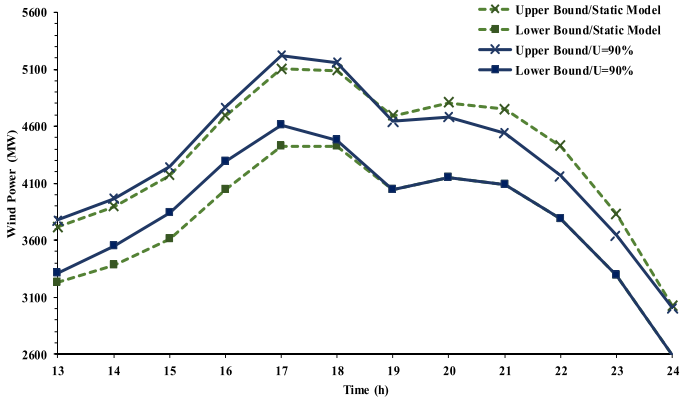

Fig. 5. Optimal upper and lower bounds provided by the proposed model with $U = 90\%$ versus the static model.

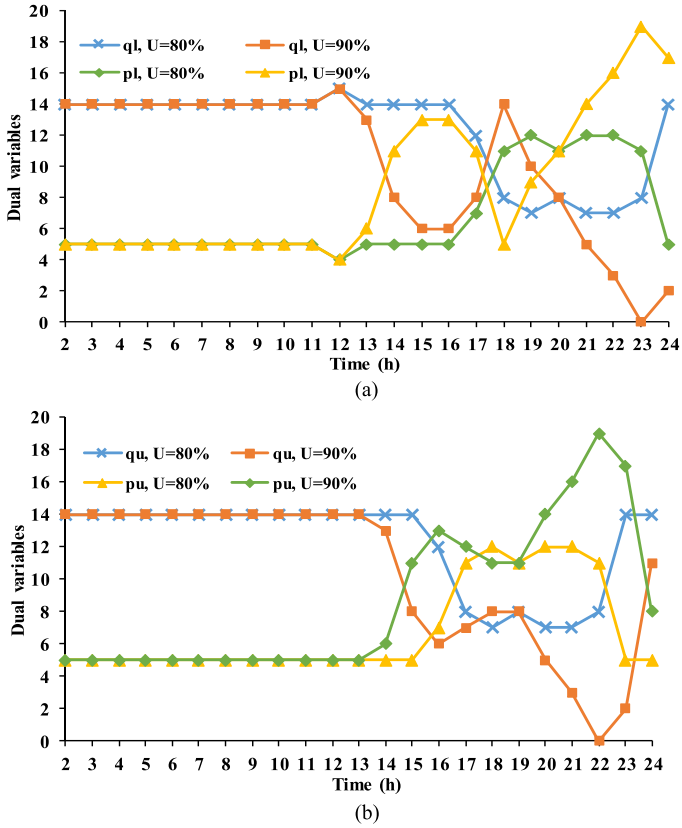

Fig. 6. Optimal dual variables of constraints (10) in (a) upward and (b) downward ramping constraints.

particularly included as little differences were observed at hours 1–12. It can be seen that the optimal uncertainty interval in the case of employing a dynamic uncertainty set ($U = 90\%$) is generally quantified narrower than that obtained from the static models.

The other observation from Fig. 4 is that the optimal uncertainty interval for the scenario of $U = 80\%$ tends more toward that where constraint (10c) is neglected compared to the obtained interval in the scenario of $U = 90\%$. It reflects that the dual variables of constraint (10c) obtained from the worst case scenarios of ramping constraints (11) when $U = 80\%$ are higher than those when $U = 90\%$. The dual variables of constraint (10c) reflect the effect of this constraint on the optimal uncertainty set. It can be also observed that the optimal uncertainty intervals at hours 1–12 for the scenarios of $U = 80\%$ and $U = 90\%$ are the same. At hours 13–17 and 20–24, the optimal interval in case of $U = 80\%$ is larger than that when $U = 90\%$. On the contrary at hours 18 and 19, the optimal interval in case of $U = 90\%$ is larger. The reason for such observations can be justified in Fig. 6 which demonstrates the optimal dual variables related to constraints (10) in the worst cases of upward and downward ramping constraints (11). In this figure, *pl* and *ql* are the dual variables corresponding to the lower limitations of (10a) and (10c), respectively, while *pu* and *qu* are the dual variables corresponding to the upper limitations. The optimal value of *qu* in the upward ramping constraint is equal to zero, whereas the optimal value of *pl* in the downward ramping constraint is zero, since β_{it} is always found negative. This figure illustrates that the optimal dual variables *ql* in two scenarios of $U = 80\%$ and $U = 90\%$ are the same at hours 1–12. Except in hours 18 and 19, the optimal *ql* for the scenario of $U = 80\%$ is higher than that when U is 90% at hours 13–24. It can be concluded that with more restrictions on the time correlation of wind generations (i.e., lower U), a larger uncertainty set is characterized. The summation of *ql* and *pl* at each hour is equal to 19. In the scenario where constraint (10c) is neglected, *pl* is almost equal to 19 at each hour. Hence, as *ql* decreases, *pl* increases due to constraints (11b), (11c), (11e), and (11f).

2) Impact of Recourse Cost on Optimal Uncertainty Interval: In dealing with uncertain conditions, even if the feasibility criterion for the operation solution is satisfied, the increased re-dispatch cost of the worst-case scenario should be limited by enforcing constraint (9). In this section, the impact of maximum recourse cost on the optimal uncertainty set is investigated. In (26), the recourse cost limitation is considered as the product of the dispatch cost under expected wind power realization and the coefficient C. The value of C is greater than 1, since the dispatch cost of generating units under uncertainty is greater than that in the base case scenario.

Fig. 7 illustrates the uncertainty set intervals corresponding to the four studied scenarios. It can be observed that as C_r

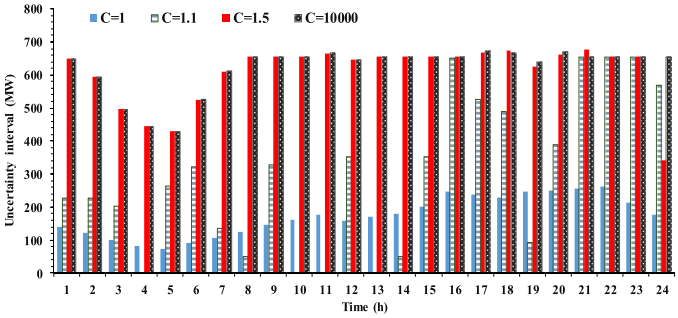

Fig. 7. Optimal uncertainty set intervals for different values of *C*.

decreases, the interval associated with the optimal uncertainty set is lower. With a larger uncertainty set, a higher re-dispatch cost will be realized. Additionally, it can be seen that the optimal uncertainty interval when coefficient *C* is higher than 1.5 remains almost constant as *C* increases. Thus, the conservativeness of the robust model can be adjusted by modifying *C* between 1 and 1.5

$$C_r = \sum_t \sum_i (c_i \overline{pg}_{it} + s_i^u \overline{u}_{it} + s_i^d \overline{v}_{it}) \times C. \tag{26}$$

3) System Operation Costs With Wind Generation Temporal Correlation Considerations: In the proposed formulation, the optimal solution is found so that the costs of LS and WS are optimized, while maintaining the model robustness. Let the renewable power generation be given by

$$pw_{wt} = \overline{pw}_{wt} + \varepsilon_{wt} \quad \forall t, \forall w. \tag{27}$$

The generating units can effectively react to the forecast errors by adjusting their outputs according to their participation factors. $\overline{pg}_{it}$ is the base point generation

$$pg_{it} = \overline{pg}_{it} + \beta_{it} \sum_w \varepsilon_{wt} \quad \forall i, \forall t \tag{28}$$

where α_{it} in the above formulations can be considered equal to $\overline{pg}_{it}$. As a result, in order to simultaneously consider the costs associated with the base-case ED, UC, LS, and WS, the following objective function is formulated:

$$\min \sum_t \sum_w \mathrm{sc}_w (W_{wt}^{\max} - W_{wt}^{\mathrm{UB}}) + lc_w (W_{wt}^{\mathrm{LB}} - W_{wt}^{\min}) + \sum_t \sum_i (c_i \alpha_{it} + s_i^u u_{it} + s_i^d v_{it}). \tag{29}$$

Table III compares the impact of dynamic uncertainty set on the operation costs in two scenarios: in the former, the optimal robust solution is obtained with objective function (1a), whereas in the latter, the objective function (29) is employed. Since the cost coefficient associated with LS is higher than that for WS, the amount of load curtailment is lower than that of WS corresponding to the optimal uncertainty set. It can be also seen that the WS cost in case of a dynamic uncertainty set is found lower than that when the wind generation temporal correlation is neglected. This is because the optimal uncertainty interval is generally quantified narrower in the case of dynamic sets as shown in Fig. 4. Moreover, implementing the proposed robust model with objective function (29) results in a higher WS cost; nevertheless, the total operation cost is reduced due to lower dispatch and commitment costs of generating units. Computation time is also lower in case of dynamic sets, since the feasible region is depleted when considering the temporal correlations of wind generation. If the objective function in the proposed model is only to minimize the ED and commitment costs along with a static uncertainty set boundaries, the flexibility capacity of the system may not be sufficient to ensure all solutions are feasible.

TABLE III
COMPARISON OF DYNAMIC AND STATIC UNCERTAINTY SET

Uncertainty Set	Objective Function	Operation Cost (k$)				Run time (s)
		ED	UC	LS	WS	
Static	(1a)	500.13	0.50	0	25.87	113
	(21)	405.21	0.27	0	31.31	84
Dynamic (U=0.9)	(1a)	500.49	0.46	9.58	25.77	86
	(21)	406.97	0.27	9.58	29.18	80
Dynamic (U=0.8)	(1a)	538.82	0.40	0	21.30	83
	(21)	408.42	0.27	0	22.48	82

TABLE IV
UNCERTAINTY SET SIZE COMPARISON

Uncertainty Set	Deviation (%)	ED (k$)	UC (k$)
Static	9	Inf.*	Inf.
	6	389.88	0.24
	5	386.87	0.23
Dynamic (U=0.9)	9	Inf.	Inf.
	6	Inf.	Inf.
	5	386.83	0.23

*Inf.: Infeasible

Table IV outlines a comparison on the size of uncertainty sets: for the deviation of 9% in case of a static uncertainty set, the system generating units have insufficient flexible ramp capability to respond leading to infeasible solutions. Providing that the uncertainty set is fixed, the solution robustness will be maintained under deviations lower than 6% for static and 5% for dynamic sets, respectively.

V. CONCLUSION

This paper suggests a novel adaptive robust optimization model based on SCUC problem with an affine-decision structure to comprehensively evaluate the operational flexibility challenges in power systems with unprecedented penetration of renewables. An efficient framework using a combination of duality theorem, C&CG, and alternative direction algorithm is developed to solve the proposed optimization model. The robust SCUC-based framework is able to capture the effect of time dependency associated with the uncertain wind generations, a type of dynamic uncertainty set, on the worst-case scenarios of generating units' ramp rate constraints (intertemporal constraints) and subsequently, on the evaluation of flexibility and dynamic uncertainty set boundaries. The suggested technique guarantees robust dispatch decisions and policies. Furthermore, the concept of recourse cost limitation is utilized to adjust the

level of decision conservativeness and the re-dispatch cost is included to accommodate the system uncertainties. Simulations on the modified IEEE RTS-96 test system revealed that the optimal uncertainty interval is generally characterized narrower in the case of dynamic uncertainty sets and the WS cost is found lower than that when the wind generation temporal correlation is neglected. Moreover, the inclusion of the recourse cost constraints demonstrates that (i) as the re-dispatch cost is further limited, the optimal uncertainty set interval is narrower and (ii) with a larger uncertainty set, a higher re-dispatch cost will be realized.

REFERENCES

[1] J. Cochran *et al.*, "Flexibility in 21st century power systems," Nat. Renew. Energy Lab., Golden, CO, USA, 2014.

[2] J. Liang, G. K. Venayagamoorthy, and R. G. Harley, "Wide-area measurement based dynamic stochastic optimal power flow control for smart grids with high variability and uncertainty," *IEEE Trans. Smart Grid*, vol. 3, no. 1, pp. 59–69, Mar. 2012.

[3] B. Zhang and M. Kezunovic, "Impact on power system flexibility by electric vehicle participation in ramp market," *IEEE Trans. Smart Grid*, vol. 7, no. 3, pp. 1285–1294, May 2016.

[4] S. Bahrami and M. H. Amini, "A decentralized trading algorithm for an electricity market with generation uncertainty," *Appl. Energy*, vol. 218, pp. 520–532, 2018.

[5] S. Bahrami, M. H. Amini, M. Shafie-Khah, and J. P. S. Catalão, "A decentralized renewable generation management and demand response in power distribution networks," *IEEE Trans. Sustain. Energy*, vol. 9, no. 4, pp. 1783–1797, Oct. 2018.

[6] NREC, "Flexibility requirements and metrics for variable generations: Implications for system planning studies," Princeton, NJ, USA, Aug. 2010. [Online]. Available at: http://www.nerc.com/files/IVGTF_Task_1_4_Final.pdf

[7] N. Menemenlis, M. Huneault, and A. Robitaille, "Thoughts on power system flexibility quantification for the short-term horizon," in *Proc. IEEE Power Energy Soc. Gen. Meet.*, San Diego, CA, USA, 2011, pp. 1–8.

[8] E. Lannoye, D. Flynn, and M. O'Malley, "Evaluation of power system flexiblity," *IEEE Trans. Power Syst.*, vol. 27, no. 2, pp. 922–931, May 2013.

[9] B. S. Palmintier and M. D. Webster, "Impact of operational flexibility on electricity generation planning with renewable and carbon targets," *IEEE Trans. Sustain. Energy*, vol. 7, no. 2, pp. 672–684, 2016.

[10] L. Zhang *et al.*, "Unified unit commitment formulation and fast multi-service LP model for flexibility evaluation in sustainable power systems," *IEEE Trans. Sustain. Energy*, vol. 7, no. 2, pp. 658–671, Apr. 2016.

[11] A. Ulbig and G. Andersson, "On operational flexibility in power systems," in *Proc. IEEE Power Energy Soc. Gen. Meet.*, San Diego, CA, USA, 2012, pp. 1–8.

[12] A. A. Thatte and L. Xie, "A metric and market construct of intertemporal flexibility in time-coupled economic dispatch," *IEEE Trans. Power Syst.*, vol. 31, no. 5, pp. 3437–3446, Sep. 2016.

[13] Z. Qin, Y. Hou, S. Lei, and F. Liu, "Quantification of intra-hour security-constrained flexibility region," *IEEE Trans. Sustain. Energy*, vol. 8, no. 2, pp. 671–684, Apr. 2017.

[14] J. Zhao, T. Zheng, and E. Litvinov, "Variable resource dispatch through do-not-exceed limit," *IEEE Trans. Power Syst.*, vol. 30, no. 2, pp. 820–828, Mar. 2015.

[15] J. Zhao, T. Zheng, and E. Litvinov, "A unified framework for defining and measuring flexibility in power system," *IEEE Trans. Power Syst.*, vol. 31, no. 1, pp. 339–347, Jan. 2016.

[16] V. K. Tumuluru and D. H. K. Tsang, "A two-stage approach for network constrained unit commitment problem with demand response," *IEEE Trans. Smart Grid.*, vol. 9, no. 2, pp. 1175–1183, Mar. 2018.

[17] D. Bertsimas, E. Litvinov, X. A. Sun, J. Zhao, and T. Zheng, "Adaptive robust optimization for the security constrained unit commitment problem," *IEEE Trans. Power Syst.*, vol. 28, no. 1, pp. 52–63, Feb. 2013.

[18] Á. Lorca and X. A. Sun, "Multistage robust unit commitment with dynamic uncertainty sets and energy storage," *IEEE Trans. Power Syst.*, vol. 32, no. 3, pp. 1678–1688, May 2017.

[19] B. Hu and L. Wu, "Robust SCUC considering continuous/discrete uncertainties and quick-start units: A two-stage robust optimization with mixed-integer recourse," *IEEE Trans. Power Syst.*, vol. 31, no. 2, pp. 1407–1419, Mar. 2016.

[20] H. Ye and Z. Li, "Robust security-constrained unit commitment and dispatch with recourse cost requirement," *IEEE Trans. Power Syst.*, vol. 31, no. 5, pp. 3527–3536, Sep. 2016.

[21] C. Shao *et al.*, "Security-constrained unit commitment with flexible uncertainty set for variable wind power," *IEEE Trans. Sustain. Energy*, vol. 8, no. 3, pp. 1237–1246, Jul. 2017.

[22] C. Wang *et al.*, "Robust risk-constrained unit commitment with large-scale wind generation: An adjustable uncertainty set approach," *IEEE Trans. Power Syst.*, vol. 32, no. 1, pp. 723–733, Jan. 2017.

[23] C. Wang *et al.*, "Risk-based admissibility assessment of wind generation integrated into a bulk power system," *IEEE Trans. Sustain. Energy*, vol. 7, no. 1, pp. 325–336, Jan. 2016.

[24] Z. Li *et al.*, "Robust look-ahead power dispatch with adjustable conservativeness accommodating significant wind power integration," *IEEE Trans. Sustain. Energy*, vol. 6, no. 3, pp. 781–790, Jul. 2015.

[25] W. Wu, J. Chen, B. Zhang, and H. Sun, "A robust wind power optimization method for look-ahead power dispatch," *IEEE Trans. Sustain. Energy*, vol. 5, no. 2, pp. 507–515, Apr. 2014.

[26] R. A. Jabr, "Adjustable robust OPF with renewable energy sources," *IEEE Trans. Power Syst.*, vol. 28, no. 4, pp. 4742–4751, Nov. 2013.

[27] J. Warrington *et al.*, "Policy-based reserves for power systems," *IEEE Trans. Power Syst.*, vol. 28, no. 4, pp. 4427–4437, Nov. 2013.

[28] L. Zhao and B. Zeng, "Robust unit commitment problem with demand response and wind energy," in *Proc. IEEE Power and Energy Soc. Gen. Meet.*, San Diego, CA, USA, 2012, pp. 1–8.

[29] C. Grigg *et al.*, "IEEE reliability test system-1996. A report prepared by the reliability test system task force of the application of probability methods subcommittee," *IEEE Trans. Power Syst.*, vol. 14, no. 3, pp. 1010–1020, Aug. 1999.

[30] H. Pandzic *et al.*, Unit Commitment Under Uncertainty - GAMS Models, Library Renew. Energy Anal. Lab, Univ. Washington, Seattle, WA, USA. [Online]. Available at: http://www.ee.washington.edu/research/real/gams_code.html

[31] [Online]. Available at: http://sina.sharif.edu/∼hosseini/Data.xls